

FY16 STATUS REPORT FOR THE URANIUM- MOLYBDENUM FUEL CONCEPT

PNNL-25846

Fuel Cycle Research & Development

*Prepared for
U.S. Department of Energy
Advanced Fuels Campaign*

*W.D. Bennett
A.L. Doherty
C.H. Henager, Jr.
C.A. Lavender
R.O. Montgomery
R.P. Omberg
M.T. Smith
R.A. Webster
September 20, 2016
FCRD-FUEL-2016-000165*



DISCLAIMER

This information was prepared as an account of work sponsored by an agency of the U.S. Government. Neither the U.S. Government nor any agency thereof, nor any of their employees, makes any warranty, expressed or implied, or assumes any legal liability or responsibility for the accuracy, completeness, or usefulness, of any information, apparatus, product, or process disclosed, or represents that its use would not infringe privately owned rights. References herein to any specific commercial product, process, or service by trade name, trade mark, manufacturer, or otherwise, does not necessarily constitute or imply its endorsement, recommendation, or favoring by the U.S. Government or any agency thereof. The views and opinions of authors expressed herein do not necessarily state or reflect those of the U.S. Government or any agency thereof.

Reviewed by:

PNNL Project Manager

Signature on file

Ronald P. Omberg

Abstract

The Fuel Cycle Research and Development program of the Office of Nuclear Energy has implemented a program to develop a Uranium-Molybdenum metal fuel for light water reactors. Uranium-Molybdenum fuel has the potential to provide superior performance based on its thermo-physical properties. With sufficient development, it may be able to provide the Light Water Reactor industry with a melt-resistant, accident-tolerant fuel with improved safety response. The Pacific Northwest National Laboratory has been tasked with extrusion development and performing ex-reactor corrosion testing to characterize the performance of Uranium-Molybdenum fuel in both these areas. This report documents the results of the fiscal year 2016 effort to develop the Uranium-Molybdenum metal fuel concept for light water reactors.

Acronyms and Abbreviations

14YWT and 9YWT	steel cladding material that has been used in liquid metal reactors
AOO	Anticipated Operational Occurrence
ATF	Advanced Test Facility
DOE-NE	U.S. Department of Energy, Office of Nuclear Energy
FCRD	Fuel Cycle Research and Development
Fe	iron
FY	fiscal year
LOCA	Loss of Coolant Accident
LWR	light water reactors
MA	mechanical alloyed
Nb	niobium
ODS	Oxide Dispersion Strengthened
OM	Optical Microscopy
PNNL	Pacific Northwest National Laboratory
psi	pounds per square inch
TE	triple extrusion
TWT	thick-wall(ed) tube
U-Mo	Uranium-Molybdenum

CONTENTS

ABSTRACT.....	IV
ACRONYMS AND ABBREVIATIONS.....	V
1. BACKGROUND OF URANIUM-MOLYBDENUM CONCEPT.....	1
2. EXECUTIVE SUMMARY OF U-MO DEVELOPMENT	3
3. ENHANCED ACCIDENT TOLERANT FUEL CONCEPT FOR LIGHT WATER REACTOR APPLICATIONS.....	5
3.1 U-Mo Fuel Design Concept Progression.....	5
3.2 Key Attributes of the U-Mo Fuel Design	5
3.3 Fabrication Process.....	6
3.4 U-Mo Rodlet Corrosion Testing.....	6
3.5 Beneficial Attributes of the U-Mo Fuel Design Concept for LWR Applications.....	7
4. FUEL/CLAD SYSTEM MANUFACTURING TECHNOLOGY DEVELOPMENT FOR U-MO FUEL DESIGN.....	9
4.1 Manufacturing Technology Development Progress	9
4.2 ODS Alloy Billet Preparation Procedure.....	12
4.3 TWT Extrusion Manufacturing Process Demonstration	12
4.4 Thermomechanical Processing of Oxide Dispersion Strengthened (ODS) Cladding.....	18
5. CORROSION TESTING AND DEVELOPMENT FOR URANIUM ALLOYS	21
5.1 Basic Images of Triple Extrusion Rod (TE1).....	21
5.2 Weld Testing.....	25
5.3 End Cap Welded U-Mo Test Sample	29
5.4 Defected Cladding for TE1 First Test	32
6. BIBLIOGRAPHY	35

FIGURES

Figure 1.1. LWR U-Mo Fuel Concept cross section	2
Figure 3.1. Schematic and pictures of rodlet.	7
Figure 4.1. 9YWT and 14YWT extrusion process.	10
Figure 4.2. MA 956 extrusion process.....	11
Figure 4.3. Machined copper tube and copper end caps with 14YWT billet.	12
Figure 4.4. Copper canned MA 956 TWT extrusion billet.....	13
Figure 4.5. Resulting MA 956 extruded rod.	14
Figure 4.6. Modified mandrel/dummy block components.....	15
Figure 4.7. Components and assembled thick-wall tubing billet.....	15
Figure 4.8. Cross section of the multi-layered co-extrusion.....	16
Figure 4.9. U-Mo and copper can prior to multi-layered co-extrusions.	17
Figure 4.10. U-Mo/Nb/stainless steel rod produced by triple extrusion.....	17
Figure 4.11. Two MA 956 extruded rods.	18
Figure 4.12. Pilger Mill (left) and high precision tube reducer (right).....	19
Figure 5.1. OM images of hand-polished cross-sections of tail and nose end of TE1	21
Figure 5.2. Higher magnification OM images of TE1 tail end in (a) and nose end in (b).....	21
Figure 5.3. OM image at 25x under polarized light showing entire polished TE1 rod end in cross-section.....	22
Figure 5.4. OM image at (a) 100x and (b) 500x showing a region of the polished TE1 rod end.....	23
Figure 5.5. TE1 Rod.....	24
Figure 5.6. Nose end of TE1 after cutting it from the main TE1 rod.	25
Figure 5.7. Basic images of weld development tests on stainless steels.....	26
Figure 5.8. Cross-sections of the six welds studied in the second weld test series. Shown in order from top to bottom are welds 1-3 in (a), welds 4 and 5 in (b) and weld 6 in (c).....	27
Figure 5.9. The second weld test series using two steel sleeves over a solid steel rod	28
Figure 5.10. Extrusion sample fitted with end caps prior to welding.	29
Figure 5.11. (a) Sample in welding fixture ready to be welded and (b) first weld.	30
Figure 5.12. OM images of welded test sample from TE1 ready to go into the autoclave test for weld integrity testing	30
Figure 5.13. (a) Welded TE1 test sample loaded into the autoclave using specimen holder stand.....	31

Figure 5.14. OM images of TE1 test sample after 165 hours in autoclave at 300°C and 1245 psi in prototypical pressurized water reactor water. 32

Figure 5.15. (a) Images of (a) rotary drill press 33

Figure 5.16. (a) Scanning electron microscope (SEM) image of cladding defect (dimple) after radial bit 34

Figure 5.17. OM images of defected (dimpled) test sample 34

TABLES

Table 5.1. TE1 dimensions at tail and nose with typical ranges 23

Table 5.2. Weld dimensions for weld study #1. 26

Table 5.3. Weld dimensions for weld study #2. 29

FY16 STATUS REPORT FOR THE URANIUM-MOLYBDENUM FUEL CONCEPT

1. BACKGROUND OF URANIUM-MOLYBDENUM CONCEPT

The primary mission of the U.S. Department of Energy's Office of Nuclear Energy is to advance nuclear power as a resource capable of meeting the nation's energy, environmental, and national security needs by resolving technical, cost, safety, proliferation resistance, and security barriers. The U.S. Department of Energy's Fuel Cycle Research and Development (FCRD) Program's focus is on long-term, science-based research and development of technologies with the potential to produce transformational changes for the nuclear fuel cycle.

The FCRD Program within the Department of Energy, Office of Nuclear Energy (DOE-NE) initiated an effort in 2010 to develop an advanced light water reactor (LWR) fuel rod concept that would provide for enhanced safety margins and increased discharge burnup levels to support improved fuel utilization in the nation's nuclear power plant fleet. One of these chosen proposals was the development of Uranium-Molybdenum (U-Mo) metal fuel for use in commercial LWRs. The U-Mo fuel rod development project was selected by DOE-NE due to the potential for this design to have; 1) physical and neutronic compatibility to the end user, 2) characteristics that are compatible with existing UO₂-based fuel assemblies, and 3) performance attributes that improve fuel utilization in LWRs. The U-Mo metal fuels may be able to provide an attractive alternative to standard fuel and Pacific Northwest National Laboratory (PNNL) has worked on providing transformational technology to be used for the development of U-Mo metal fuel for use in commercial LWRs.

Following the events at the Fukushima Daiichi power plants in the aftermath of the Great East Japan Earthquake and tsunami on March 11, 2011, the FCRD Program shifted focus to the development of Enhanced Accident Tolerant Fuel concepts. The goal of these concepts is to tolerate loss of active cooling in the reactor core for a considerably longer time period than the standard UO₂-Zircaloy system while maintaining or improving fuel performance during normal operation, and operational transients, as well as design basis and beyond design basis events. The U-Mo fuel design development effort has continued after this shift in focus by DOE-NE, due in large part to the substantial improvement in fuel rod behavior during design basis accidents, such as the Loss of Coolant Accident (LOCA) and the Reactivity Initiated Accident that this design affords.

A suggested approach is the development of heterogeneous metallic uranium alloys that contain a diffused surface layer for improved surface corrosion resistance. Surface alloying consists of aluminum, niobium, chromium, and/or platinum diffused into the outer surface of the uranium metal fuel rod for a coating that will withstand loading into the cladding during fabrication and provide superior corrosion resistance during accident scenarios. Several uranium metal alloys have been investigated over the last few decades and there is ample evidence that various metal fuel alloys can be developed that will significantly reduce the metal-water reaction, and hydride formation. These studies show that the addition of small amounts of aluminum, niobium,

chromium, and/or platinum to a U-Mo alloy could achieve reduced metal-water interactions [2]. The small additions of aluminum may also be beneficial insofar as phase stability is concerned. The schematic of the major components of the LWR U-Mo Fuel Concept is shown in Figure 1.1.

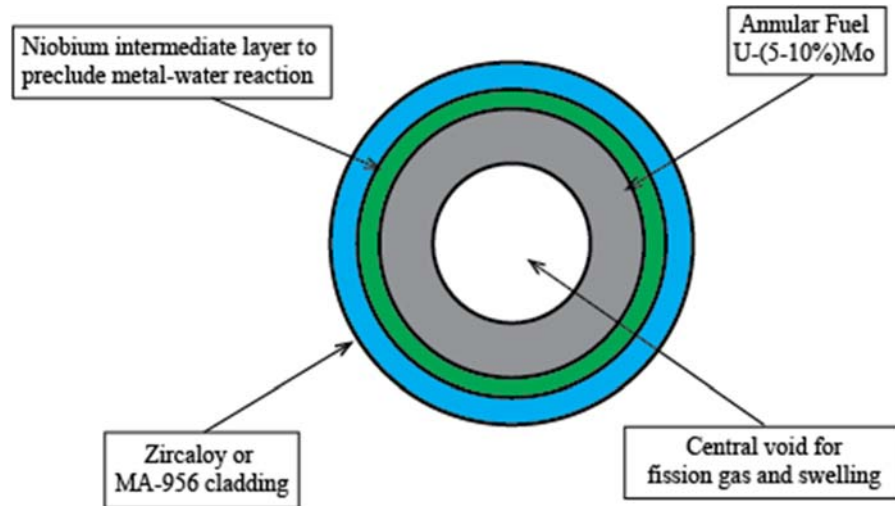


Figure 1.1. LWR U-Mo Fuel Concept cross section (not to scale).

The annular U-Mo fuel region contains 5% to 10% molybdenum in metal form enclosed within a multi-layer cladding composed of an inner layer of niobium and external layer of either Zircaloy or FeCrAl materials. The intermediate niobium (or other candidate material) layer is placed between the fuel material and the cladding to preclude any reaction between the U-Mo metal and the surrounding water in the event of a cladding breach. This liner also minimizes any chemical reactions between the fuel material, volatile fission products, and the cladding. The design has a central void that functions as a fission gas plenum and to accommodate irradiation swelling of the fuel.

The fuel rod design is fabricated using a multi-layer extrusion and pilgering process that produces metallurgical bonding between the individual component layers, providing enhanced heat transfer properties, structural integrity, and chemical stability. PNNL has been focused on the development of extrusion techniques and the reaction between metal U-Mo and water. This report for the fiscal year (FY)16 will summarize the U-Mo concept and the multiple alternative cladding concepts that are being explored. The process for selection of cladding material is based on selecting the material that will provide the most advantageous behavior in the event of a LOCA.

2. EXECUTIVE SUMMARY OF U-MO DEVELOPMENT

This report documents the continued development of the extrusion processes and techniques. PNNL is also supporting the Advanced Test Facility (ATF-1 Test) by developing a pilgering process for alternate oxide dispersion strengthened (ODS) cladding such as 14YWT, 9YWT and MA (Mechanical Alloyed) 956. The desire is to be able to produce multi-layered extrusions that will produce a tube that can be cold reduced and annealed for the ATF-1 Test.

This report also documents and assesses the impacts that continued alloy development can have on the improvement in corrosion rates for U-Mo alloys that can potentially provide an improved accident-tolerant metal fuel.

3. ENHANCED ACCIDENT TOLERANT FUEL CONCEPT FOR LIGHT WATER REACTOR APPLICATIONS

3.1 U-Mo Fuel Design Concept Progression

The DOE is developing a U-Mo metal alloy Enhanced Accident Tolerant Fuel concept for Light Water Reactor applications that provides improved fuel performance during normal operation, anticipated operational occurrences, and postulated accidents. The high initial uranium atom density, the high thermal conductivity, and a low heat capacity permit a U-Mo-based fuel assembly to meet important design and safety requirements. These attributes also result in a fuel design that can satisfy increased fuel utilization demands and allow for improved accident tolerance in LWRs.

This fiscal year status report for the U-Mo Fuel Concept summarizes the results obtained from the on-going activities to; 1) produce a multi-layered extrusion of stainless steel cladding/niobium liner/U-10Mo fuel rod specimen and 2) test the high temperature water corrosion of rodlet samples containing a drilled hole in the cladding. The results from corrosion testing will be discussed which yield insights into the resistance to attack by water ingress during high temperature water exposure for the multi-layered extruded samples containing a drilled hole, simulating a cladding failure.

These preliminary evaluations indicate that the U-10Mo fuel design concept has many beneficial features that can meet or improve conventional LWR fuel performance requirements under normal operation, AOOs, and postulated accidents. The viability of a deployable U-Mo fuel design hinges on demonstrating that fabrication processes and alloying additions can produce acceptable irradiation stability during normal operation and accident conditions and controlled metal-water reaction rates in the unlikely event of a cladding perforation. In the area of enhanced accident tolerance, a key objective is to establish that the lower stored energy of the U-Mo fuel design can provide the emergency core cooling systems the opportunity to maintain the reactor core in an easier to cool geometry following an accident.

3.2 Key Attributes of the U-Mo Fuel Design

The principal attributes of the U-Mo fuel system are its high initial uranium atom density, the high thermal conductivity, and a low heat capacity. These characteristics permit a fuel assembly based on U-Mo material to meet important design requirements such as fissile atom density, fuel rod diameter and length, and assembly rigidity and weight, while delivering improved thermal and mechanical performance during normal operation. Compared to oxide fuel, the higher thermal conductivity yields lower fuel temperatures and greater heat removal capability. These aspects are conducive to a fuel design that can replace UO₂ and meet the fuel assembly geometric and structural requirements (transparency) and potentially allow for improved accident behavior and future power upgrades for LWRs.

Corrosion studies of the metal water reaction of both bare and clad uranium alloys have found:

1. Under conditions of bare metal exposure to high temperature water, these alloys exhibit smooth corrosion layer formation that flakes off during exposure (sloughing) with a thin protective layer that exhibits an approximately constant thickness.
2. For long exposure times (days to weeks), a second process occurs where excessive hydrogen absorption initiates due to breakdown of the protective oxide. This leads to extensive cracking of the metal and loss of structural integrity.
3. In the case of clad samples with defects, corrosion behavior is controlled first by the bond between the fuel and the cladding and then second by the microstructure and/or alloy content.
4. Zirconium alloy cladding was also found to reduce hydrogen uptake in some uranium alloys by acting as a hydrogen getter. The ability of the cladding to serve as a hydrogen getter is an important component of reaching long time corrosion stability of this fuel design.

3.3 Fabrication Process

The approach to fabricate the U-Mo LWR fuel concept consists of three main stages; source material preparation and billet fabrication, hot mechanical co-extrusion of multi-layer materials, and final pilgering to dimensional and microstructure requirements. The co-extrusion/pilgering process is attractive for two reasons; the metallurgical bond between the fuel material and cladding, and the potential to construct a commercially viable fabrication capability.

The multi-layered extrusion and fabrication process demonstration results shown in Section 4 and 5 demonstrate that rod billets composed of these three materials can be extruded successfully into suitable rod geometries with evidence of metallurgical bonding between all the different materials. Both the interface regions and the material thicknesses exhibit non-uniform features that arise from source material inhomogeneity and spatially varying stress fields during the extrusion procedure. Further optimization is needed in the areas of source material microstructure homogeneity, reduction of impurity content, and extrusion rates/temperatures to improve the uniformity of the metallurgical bonds and the liner and cladding thickness. Samples have been removed from this rod for high temperature water corrosion testing as discussed in the following section.

3.4 U-Mo Rodlet Corrosion Testing

An important focus of the U-Mo LWR fuel development activities is identifying outer fuel surface alloying techniques and/or liner materials that will improve the corrosion resistance of this fuel design in the event that the cladding is breached.

The corrosion test method examined consists of an integral fuel/liner/cladding test to exam the effectiveness of the fuel and clad system in mitigating the consequences of exposure of the fuel material to high temperature water in the presence of a defect. Various physical mechanisms are thought to influence the stability of the integral rod in corrosion, including hydrogen gettering by the cladding and occluding of the cladding defect. This proof-of-principle test uses a short rodlet specimen of extruded U-Mo fuel, liner, and cladding containing a pre-drilled defect. The sample is exposed to high temperature and pressure water containing dissolved boron and lithium within an environmentally controlled autoclave system for extended time periods.

A schematic of the proof-of-principle test sample is shown Figure 3.1 along with a photo of an actual test rodlet. The test specimen consists of a short multi-layered extruded rod with welded endcaps. A pre-drilled dimple is used to simulate a defect in the cladding. This dimple allows for water to react with the inner liner material and/or the U-Mo material.

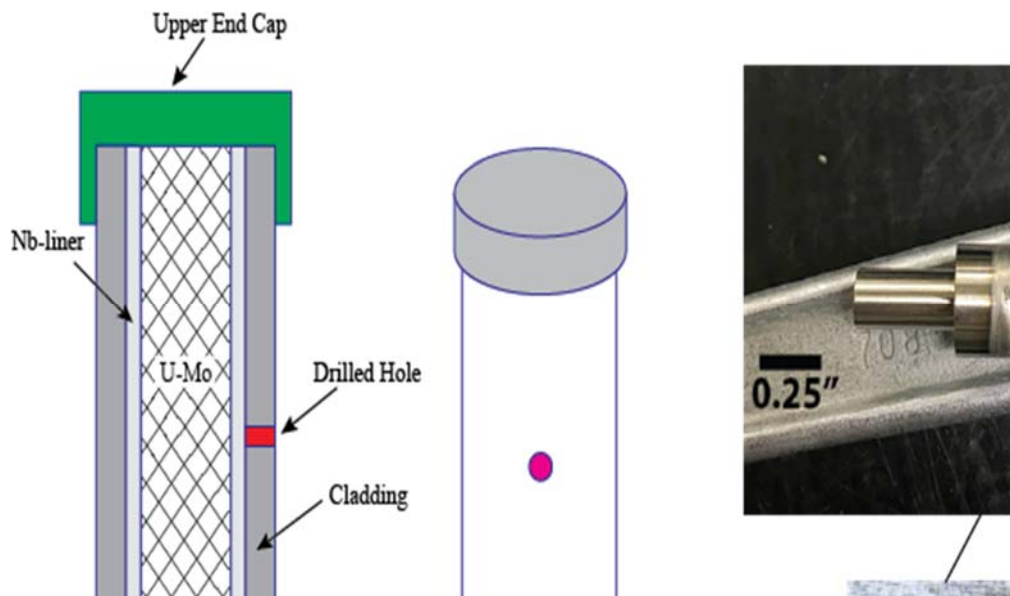


Figure 3.1. Schematic and pictures of rodlet.

3.5 Beneficial Attributes of the U-Mo Fuel Design Concept for LWR Applications

The DOE is developing a U-Mo ATF concept for LWR applications that provides improved fuel performance during normal operation, anticipated operational occurrences, and postulated accidents. The key features of the U-Mo fuel rod concept are a uranium fuel with 10% molybdenum in metal form enclosed within a multi-layer cladding composed of an inner layer of niobium and external layer of either Zircaloy or FeCrAl materials. The fuel geometry is annular with a central void employed for the retention of fission gas and fuel material swelling. The fuel rod design is fabricated using a multi-layered extrusion process that produces metallurgical bonding between the three material layers, providing both structural integrity and chemical stability.

The proposed U-Mo fuel design configuration has many beneficial attributes as an advanced LWR fuel concept. These are; 1) the ability to meet important design requirements such as fissile atom density, fuel rod diameter and length, and assembly rigidity and weight, 2) improved thermal performance during normal operation leading to reliable operation, enhanced operational flexibility, and improved safety margin for many AOOs and operational transients, and 3) the reduced stored energy can result in important changes in the core response during a LOCA, leading to lower temperatures, mitigation of hydrogen generation, improved core reflooding rates, and repurposing of reactor cooling system (RCS) coolant for long-term cooling.

The recent U-Mo fuel development activities have demonstrated that; 1) the metal-water reaction in the U-Mo material can be reduced by optimization of the fuel microstructure and use of an intermediate niobium layer or surface alloying treatment, 2) the multi-material extrusion fabrication processes can produce metallurgical bonding at interfaces between U-Mo and niobium or zirconium materials, and 3) the integral rodlet corrosion samples can be fabricated with drilled holes to evaluate the ability of the fuel-cladding system to mitigate corrosion reactions. Scoping calculations have identified that the reduced stored energy of the U-Mo fuel at the initiate on of a LOCA event may reduce core temperatures below 500-600°C during the early phase of the LOCA event. The viability of a deployable U-Mo fuel design hinges on demonstrating acceptable metal-water reaction during normal operation in the unlikely event of a cladding perforation and on providing the safety systems the opportunity to maintain the reactor core with improved cooling capability following an accident.

4. FUEL/CLAD SYSTEM MANUFACTURING TECHNOLOGY DEVELOPMENT FOR U-MO FUEL DESIGN

This section describes the processes demonstrated, tooling used, and techniques developed for U-Mo fuel design.

4.1 Manufacturing Technology Development Progress

The following two figures depict the manufacturing process steps that were demonstrated (in green) and that are planned (in yellow) for 14YWT, 9YWT, and MA 956 cladding materials respectively. These process steps are grouped into three phases as shown in Figure 4.1 and Figure 4.2.

Phase 1 is the multi-layered-billet preparation, followed by the billet extrusion to an intermediate thick-walled tube (in Phase 2). Finally, Phase 3 takes the intermediate thick-walled tube reduction to its final reduction size.

9YWT/14YWT Extrusion Process

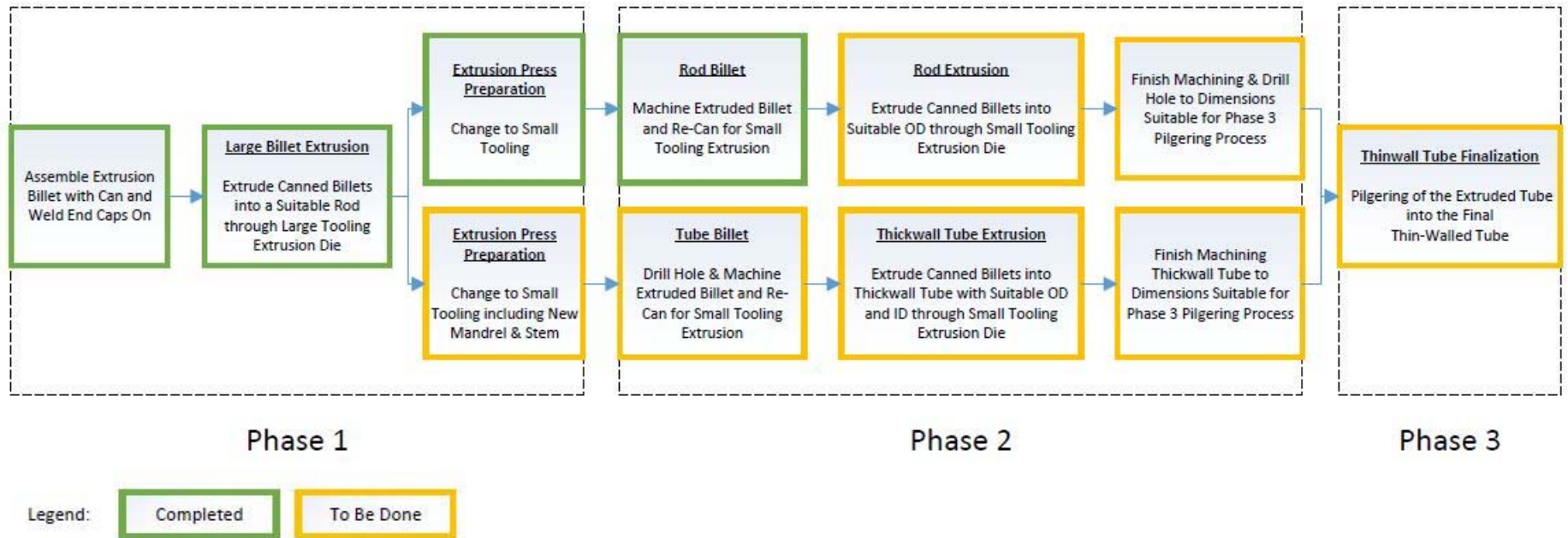


Figure 4.1. 9YWT and 14YWT extrusion process.

MA956 Extrusion Process

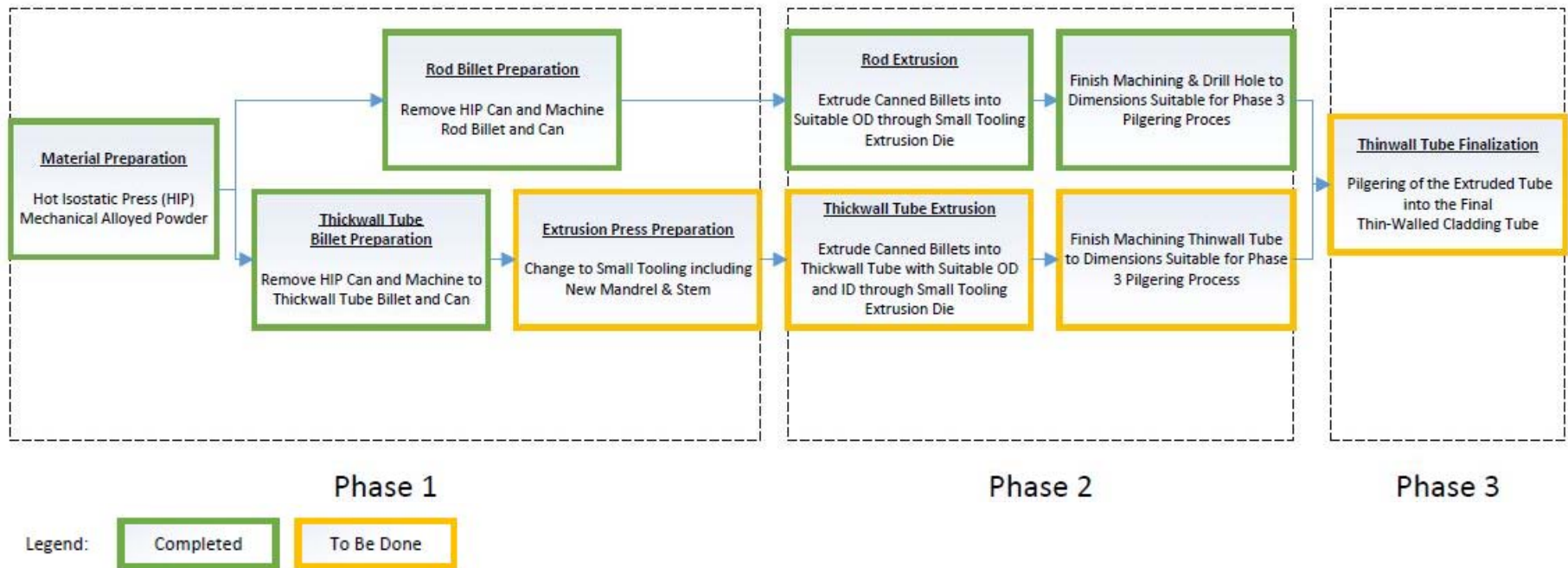


Figure 4.2. MA 956 extrusion process.

4.2 ODS Alloy Billet Preparation Procedure

The successful development of new iron (Fe) based cladding materials requires the ability to extrude billets of the material. During FY16 PNNL received samples of ODS alloy materials (14YWT and 9YWT) for preparation into extrusion billets that could be processed into solid rod or thick-wall tube (TWT) forms. In order to maximize the amount of material that could be processed into cladding tube form, the YWT materials were first extruded through the large PNNL extrusion tooling and then subsequently prepared into TWT billets for extrusion through the standard size PNNL extrusion tooling. For the purpose of this report the large extrusion process will focus on the single 14YWT billet that was machined from solid rod material. An additional 14YWT and a single 9YWT were prepared from TWTs that required that a stainless steel plug be machined to fit the hollow inner diameter. The two billets with the stainless steel plugs were extruded successfully but are not representative of the large diameter extrusion process.

The solid 14YWT material was machined into billet form and encapsulated in a copper can for extrusion. Figure 4.3 shows the billet and the copper can components prior to extrusion. The billet was then assembled and extruded through the large PNNL extrusion tooling to produce a solid rod extrusion using a relatively low extrusion ratio. After extrusion the copper can was removed by chemical etching. The bare 14YWT extruded rod was then machined to a uniform outside diameter for subsequent extrusion through the standard PNNL extrusion tooling. The extrusion of the billet through the large extrusion tooling resulted in enough material to machine two billets for use in the TWT extrusion demonstration.



Figure 4.3. Machined copper tube and copper end caps with solid 14YWT billet.

4.3 TWT Extrusion Manufacturing Process Demonstration

The successful development of new Fe based cladding materials also requires the ability to extrude billets of the material directly to a TWT. During the FY16 extrusion manufacturing process, tasks were conducted to demonstrate the ability to extrude a TWT from MA 956 and the 14YWT and 9YWT Fe-based alloys. The process steps that were demonstrated during FY16 are

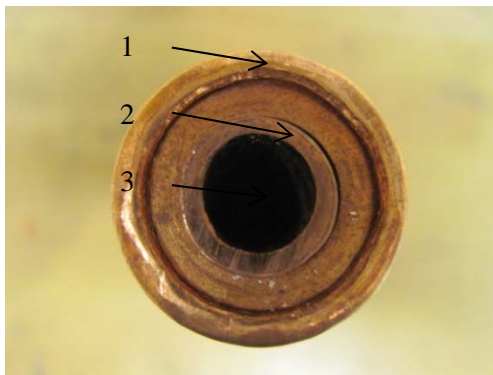
shown in green and detailed in Figure 4.1 and Figure 4.2 for 14YWT, 9YWT, and MA 956 cladding material respectively.

4.3.1 MA 956 Tube Extrusion

This section describes the TWT extrusion attempt and the redesign and procurement of new tooling for further extrusion work.

4.3.1.1 Thick-Wall Tubing Extrusion

The initial attempt to demonstrate a TWT extrusion utilized a billet of MA 956 with an internal hole bored through the billet. The TWT billet was encapsulated in a copper can with end caps and a thin-wall copper tube located in the internal bore. The billet assembly is shown in Figure 4.4.



Cu canned MA 956 extrusion billet

1. Swaged Cu tube used for outer can
2. Sized Cu tube used for inner can
3. Cu washers used for end caps

Figure 4.4. Copper canned MA 956 TWT extrusion billet.

The initial extrusion tooling approach for the TWT demonstration utilized a floating mandrel and a graphite dummy block. The mandrel and graphite assembly were then inserted into the internal bore of the MA 956 billet prior to the assembly being loaded into the extrusion container and extruded. Although the MA 956 billet extruded successfully, the floating mandrel failed inside the extruded tube and could not be removed. Examination of the extrusion and mandrel indicated that the steel mandrel was heated by the high temperature MA 956 billet material, significantly lowering the yield strength of the mandrel and thus failing under the high hydrostatic extrusion pressure. The resulting extruded MA 956 rod is shown in Figure 4.5.

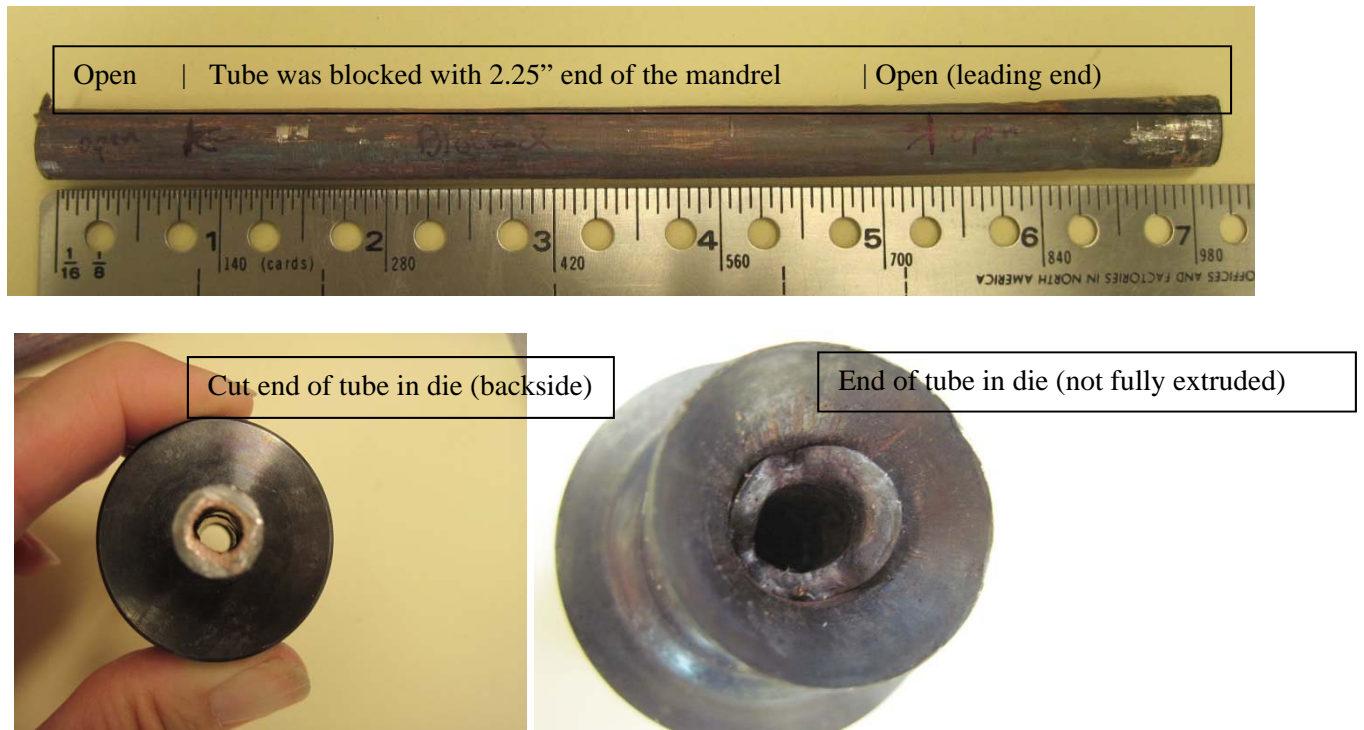


Figure 4.5. Resulting MA 956 extruded rod.

4.3.1.2 Redesign and Procurement of New Tooling

Following the evaluation of the mandrel failure, it was decided to redesign the mandrel and dummy block tooling prior to any additional TWT extrusion attempts. To reduce the heating of the mandrel material during extrusion, new tooling was designed that combines the mandrel stem with the steel dummy block into a single part which is then mechanically attached to the extrusion stem. The purpose of the design is to allow the heated billet to be placed on the loading tray without the mandrel being inside the billet. This is intended to keep the steel mandrel at room temperature and avoid heating it prior to the extrusion. In addition the attachment of the mandrel to the stem through a threaded stud allows the mandrel to be retracted out of the TWT after it clears the extrusion die. To assist in retracting the mandrel, the new mandrel design incorporates a dimensional taper over the length of the mandrel stem.

The new tooling was designed and a subcontract placed for fabrication, including several spare mandrels having two different nominal diameters. The modified mandrel/dummy block components and stems are shown in Figure 4.6.



Figure 4.6. Modified mandrel/dummy block components.

Because the new mandrel design is mechanically attached to the stem and not inserted into the hot billet at the time of extrusion, it was necessary to modify the TWT billet design and reduce the overall length of the billet to approximately 2.0 inch. Figure 4.7 (a) and (b) show the components of the TWT billet that utilize the modified billet design. Figure 4.7 (c) shows the TWT billet assembled with those components prior to crimping the ends.

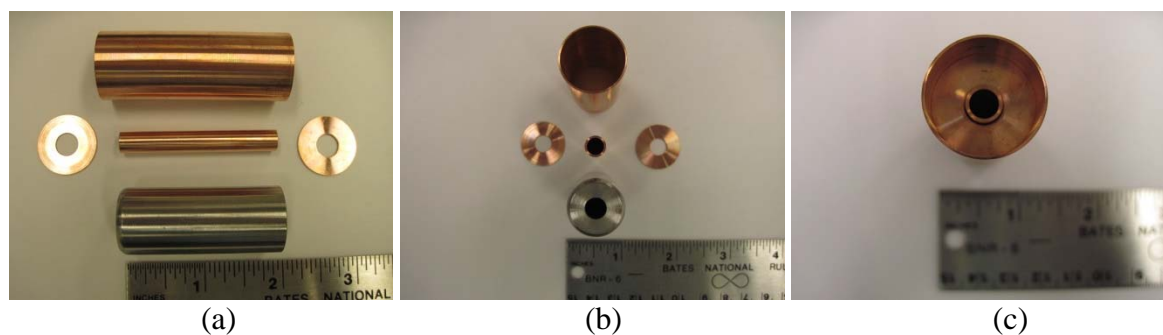


Figure 4.7. Components and assembled thick-wall tubing billet.

Following receipt of the redesigned tooling and assembly of the MA 956 and 14YWT billets, a number of practice loading runs were conducted to optimize the handling of the new billets and to reduce loading time to prevent additional heating of the mandrel assembly. The practice runs also verified that the mandrel will safely engage into the internal bore of the TWT billet at high ram travel speeds.

4.3.2 Extrusion of the Double Clad U-10 Mo Billets (with Nb & SS)

A second task conducted during FY16 was first to demonstrate the extrusion of a solid U-10Mo billet having two co-extruded cladding layers. For the solid element U-10Mo fuel, a key technical issue is its corrosion behavior under conditions where the outer cladding develops a defect, flaw, or pinhole exposing the U-Mo to coolant water. In addition, the proposed use of new Fe-based claddings may require an intermediate material layer between them and the U-Mo fuel element to prevent reaction during high temperature extrusion and the subsequent fuel element reactor conditions.

The multi-layered extrusion will involve U-Mo surrounded by an inner layer and then a cladding layer as shown in Figure 4.8.

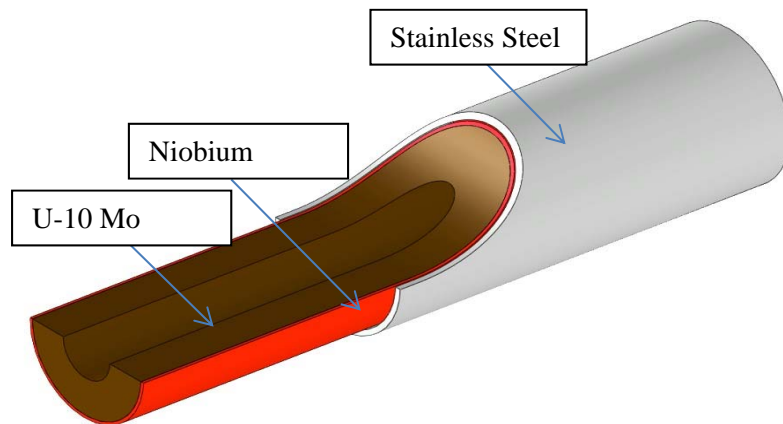


Figure 4.8. Cross section of the multi-layered co-extrusion.

4.3.2.1 Design, Assembly, and Extrusion

For the double clad extrusion demonstration a number of calculations were conducted to determine the optimum thickness of the outer cladding layer and the intermediate clad layer in contact with the U-Mo. Previous studies indicated that niobium (Nb) can provide superior corrosion protection for uranium [2]. Based on available commercial Nb materials a thin-wall clad tube was selected and the U-10Mo billet machined to fit the inner diameter of the Nb tube. For the double clad extrusion demonstration 306 stainless steel tube was used for the outer cladding layer and machined to closely fit the Nb tube outer diameter. The individual components of the double clad billet are shown in Figure 4.9.

Following successful extrusion of the double clad billet into rod form, the outer copper can was removed by chemical etching and the front and tail ends of the rod were sectioned off to provide a cross section of the double clad rod.



Figure 4.9. U-Mo and copper can prior to multi-layered co-extrusions.

Figure 4.10 shows the extruded U-Mo/Nb/Stainless steel rod and the optical metallograph of cross section as well as the scanning electron microscope image of the material interfaces.

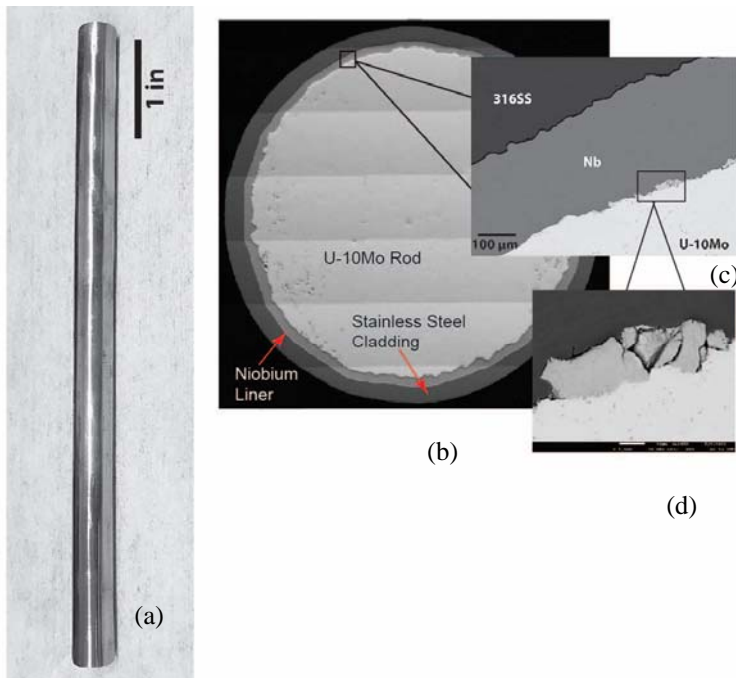


Figure 4.10. U-Mo/Nb/stainless steel rod produced by triple extrusion.

(a) polished 6" rod after extrusion, (b) optical metallograph of cross section showing all three materials, (c) scanning electron microscope image of the U-Mo/Nb interface and the Nb/SS interface, and (d) U-Mo/Nb interface reaction particle.

4.4 Thermomechanical Processing of Oxide Dispersion Strengthened (ODS) Cladding

As part of the activity to fabricate tubing for cladding from difficult to fabricate materials, PNNL is fabricating MA 956, 14YWT, and 9YWT for the Los Alamos National Laboratory. The process being employed is to initially extrude billets into annular tubes (called hollows) and then to subsequently cold work the extruded hollows to a final size consistent with LWR cladding. In a joint effort with a commercial tube manufacturer, PNNL will perform cold working and annealing trials on the three oxide dispersion strengthened (ODS) grades (MA 956, 14YWT, and 9YWT).

The MA 956 material is an iron-based high temperature alloy produced by a mechanical alloying process involving high energy ball milling of Fe and alloying elements. The MA process introduces a certain percentage of distributed oxygen into the resulting powder which improves elevated temperature strength and properties. At the same time, the oxygen and alloy composition of MA 956 results in relatively high strength at elevated temperatures, which in turn, requires higher extrusion forces. During the extrusion development and demonstration phase, a number of technical challenges were encountered. The high elevated temperature flow stress of MA 956 required that the extrusion be run at the highest possible temperature in order to reduce the flow stress. Two MA 956 extruded rods were successfully processed during the extrusion phase of the MA 956 manufacturing demonstration using a copper canned billet as shown in Figure 4.11.



Figure 4.11. Two MA 956 extruded rods.

4.4.1 Pilgering Process

Currently, PNNL is evaluating the use of two technologies: cold pilgering and tube reducing for producing tubes with the desired wall thickness. Both manufacturing processes are commercially available and utilized for producing seamless tubes in a variety of alloys.

Figure 4.12 provides an example of both technologies.

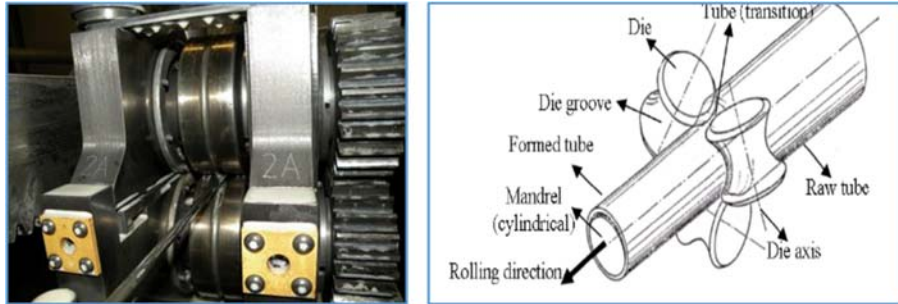


Figure 4.12. Pilger Mill (left) and high precision tube reducer (right).

These two technologies (pilgering & tube reducing) are similar in principle as a set of dies is utilized to reduce the outer diameter, while a mandrel positioned in the inner diameter is utilized for producing the desired wall thickness. In each case, both processes are discontinuous and a small increment of material is fed into the roll stand, elongated, and then rotated and the cycle repeated for each stroke. Pilgering and tube reducing differ in that pilgering is generally considered more versatile regarding the range of input/output dimensions, while the design of tube reducing tooling is less complex than pilgering. Both processes differ from drawing in that the material is formed in compression vs. tension allowing for higher area reductions. PNNL will select one of these two technologies and demonstrate the feasibility of cold working MA 956, 14YWT, and 9YWT over a range of area reductions to assess the impact on properties and microstructure, and demonstrate the feasibility of producing tubes with wall thicknesses representative of typical LWR cladding.

4.4.2 Annealing Process

In addition to evaluating the cold formability of the ODS alloys under consideration, PNNL will work to optimize the thermomechanical processing by assessing the impact of anneal temperature and degree of cold work on microstructure and mechanical properties of the alloys. Additionally, samples taken from tubes processed with various area reductions will be utilized for developing a recovery curve for each alloy.

5. CORROSION TESTING AND DEVELOPMENT FOR URANIUM ALLOYS

5.1 Basic Images of Triple Extrusion Rod (TE1)

The extruded rod shown in Figure 4.11 is referred to as TE1 for triple extrusion #1 and consists of U-Mo/Nb/Stainless Steel with the center portion of the rod extruded U-Mo and with an intermediate Nb layer with an outer stainless steel cladding. See Table 5.1 for details and the range of dimensions. Optical Microscopy (OM) images are shown in Figure 5.1. Figure 5.1(a) shows an OM image of the tail end of extrusion TE1 and (b) is a similar image of the nose end of TE1. The outer stainless steel, inner Nb, and U-10Mo meat are clearly visible. There is less faceting of the Nb layer and more uniformity in the layer thicknesses in the tail end of TE1.

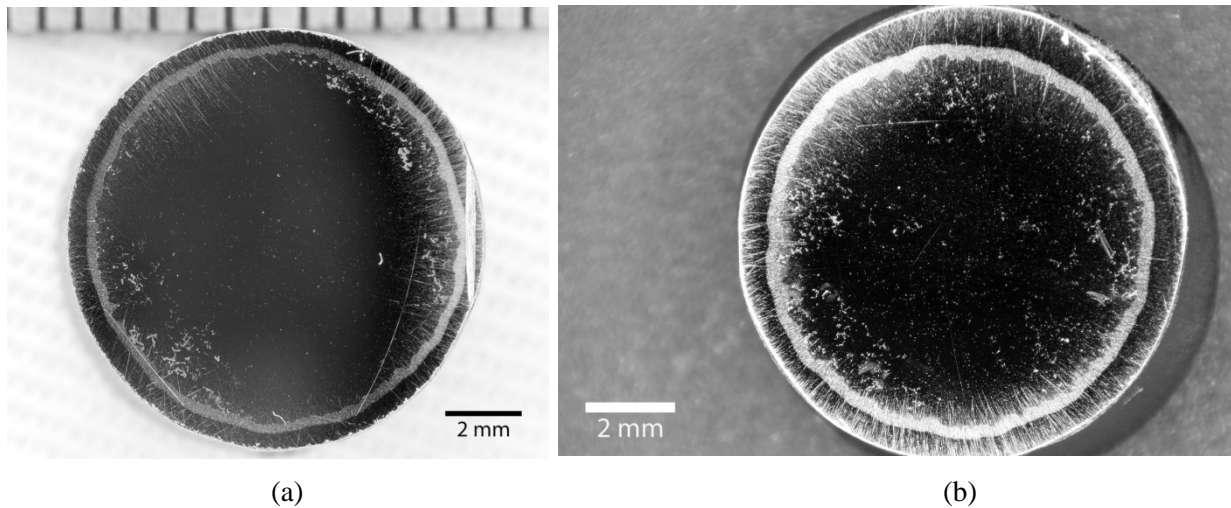


Figure 5.1. OM images of hand-polished cross-sections of tail and nose end of TE1. Shown in (a) is the tail end cross-section while (b) is the nose end.

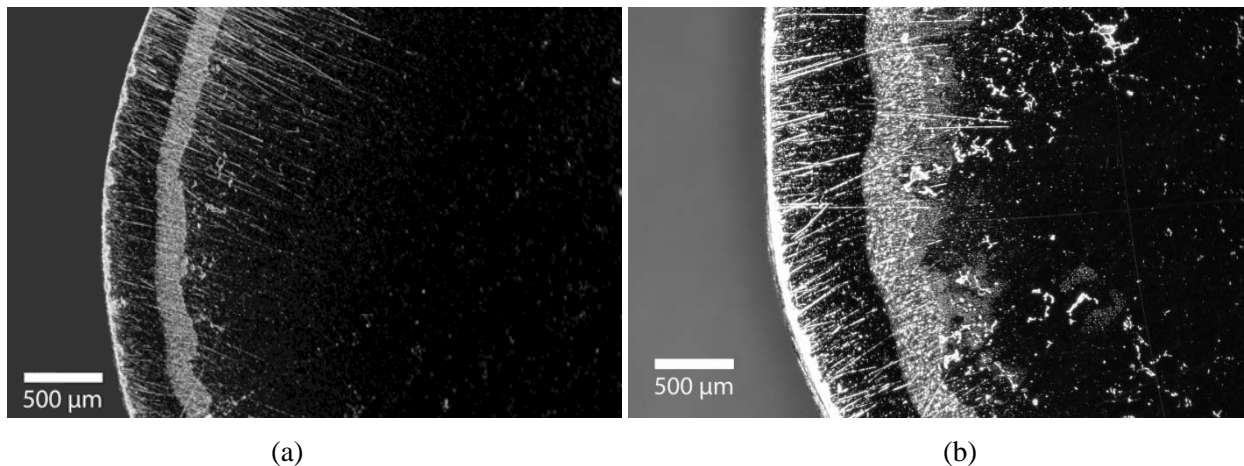


Figure 5.2. Higher magnification OM images of TE1 tail end in (a) and nose end in (b).

There is good bonding with the U-10Mo fuel meat and each layer with the other. The entire extrusion is slightly eccentric, which is not specifically quantified. The outer surface is quite smooth but the surface roughness is not quantified. The inner Nb layer is noticeably faceted on its inner diameter and exhibits some sharp peaks in thickness. The outer diameter is much smoother than the inner and this is likely due to the strong texture of the bounding U-10Mo fuel meat during the extrusion process causing non-uniform flow. This can be addressed by cold working and reducing the U-10Mo billets prior to final extrusion with the dual cladding layers.

5.1.1 Optical Microscopy of Polished TE1

Sections of TE1 that were only hand polished were finished with colloidal silica polishing cloths for more detailed images of the extrusion cross-sections. An overview OM image taken under polarized light is shown in Figure 5.3. The dark regions visible in the U-Mo are carbide and silicide inclusions. Higher magnification polarized light OM images are shown in Figure 5.4, where the U-Mo grain structure and inclusions are more visible. As seen in other studies of this U-Mo alloy, the U-Mo grain boundaries are decorated with carbide and silicide inclusions from the original cast material.

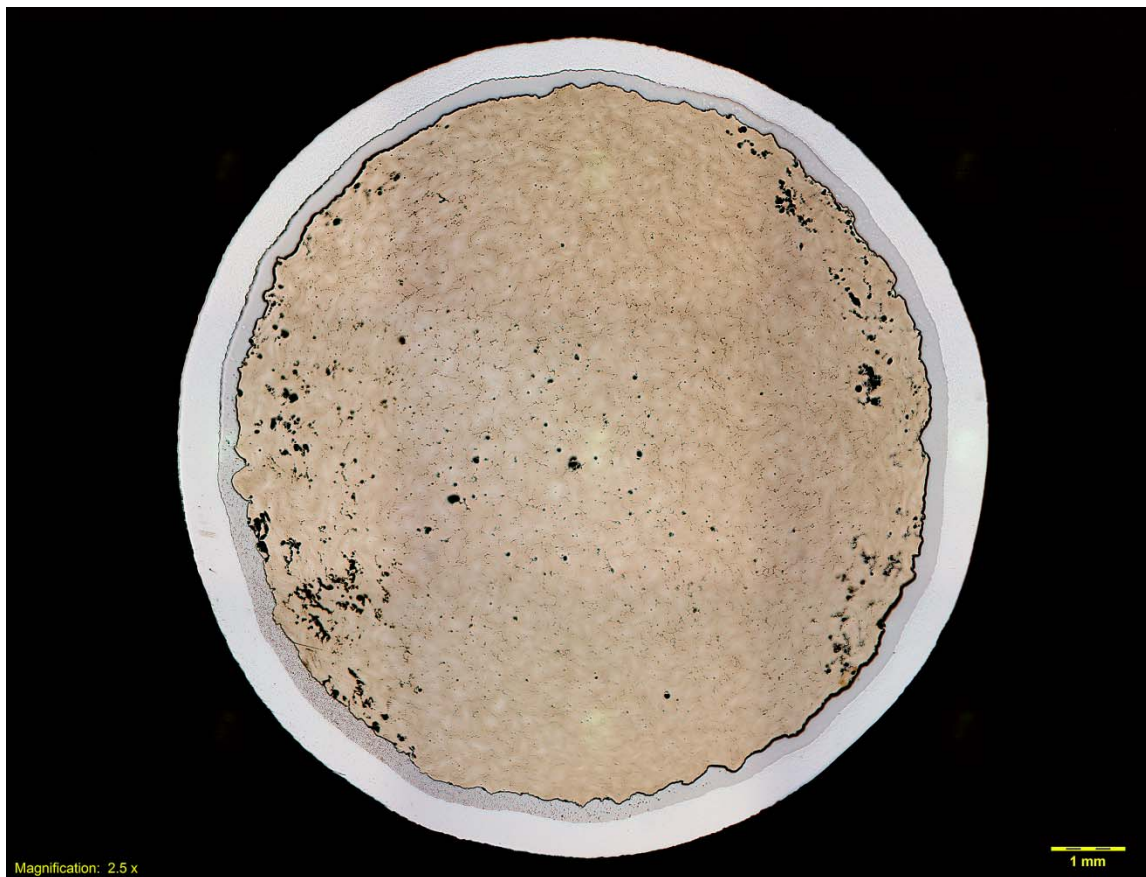


Figure 5.3. OM image at 25x under polarized light showing entire polished TE1 rod end in cross-section.

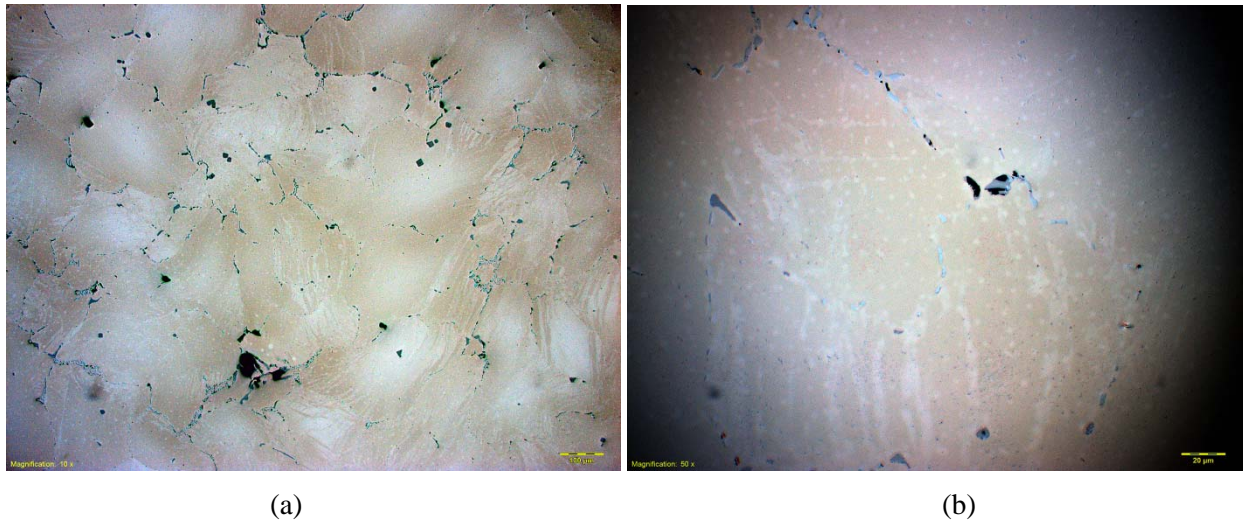


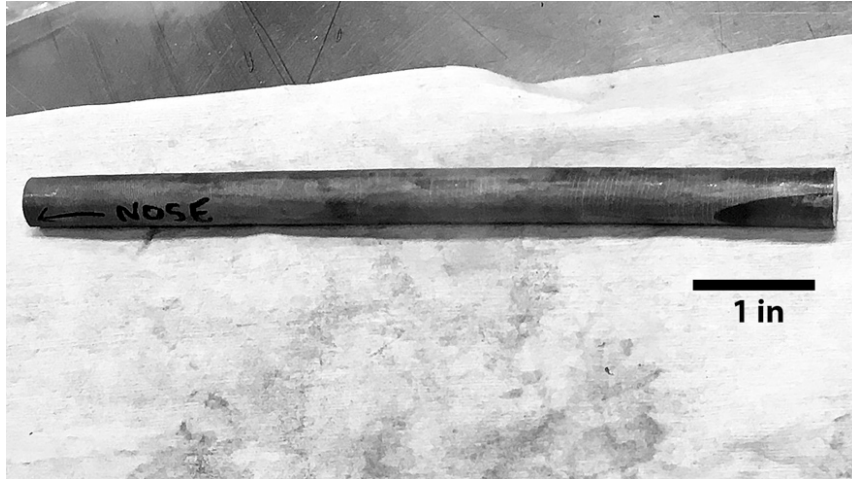
Figure 5.4. OM image at (a) 100x and (b) 500x showing a region of the polished TE1 rod end.

Table 5.1. TE1 dimensions at tail and nose with typical ranges.

Layer	Tail End TE1	Nose End TE1
Outer Steel	273-519 μm (10.7-20.4 mils)	440-980 μm (17-39 mils)
Nb	164-383 μm (6.45-15.1 mils)	165-440 μm (6.5-17 mils)
Total	11.2 cm (0.44 in)	10.4 cm (0.41 in)

5.1.2 Polishing the TE1 Rod for Autoclave Testing

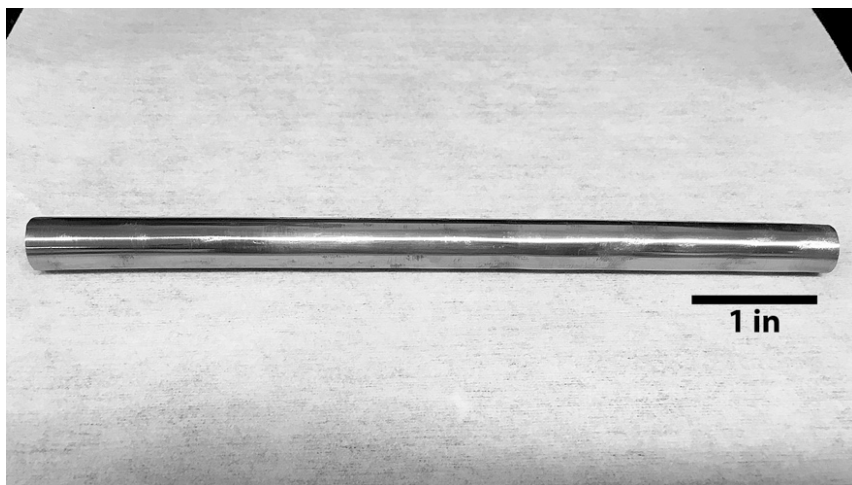
The TE1 rod was mounted in a tabletop lathe and polished by hand sanding to 1200-grit finish. The multi-layered extrusion rod after Cu and end tailings removal and before polishing is shown in Figure 5.5(a). The rod mounted in a tabletop lathe for hand polishing using SiC-grit papers is shown in Figure 5.5(b). The setup shown is in a contamination area set up for radioactive metal preparation steps. Shown in Figure 5.5(c) is the finished rod with polished outer stainless steel clad layer finished down to 1200 grit, which is suitable for end cap welding.



(a)



(b)



(c)

Figure 5.5. TE1 Rod after (a) extrusion and Cu-removal, (b) mounting in lathe, and (c) surface polishing to 1200-grit finish.

5.1.3 TE1 Nose End Removal for Weld Testing

A one-inch long section of the nose of TE1 was cut from the rod for weld testing. The nose end was slightly smaller in diameter compared to the tail end and was more tapered than the majority of the TE1 rod. Figure 5.6 shows the nose end after cutting and the image is annotated with minimum and maximum diameter measurements.



Figure 5.6. Nose end of TE1 after cutting it from the main TE1 rod.

5.2 Weld Testing

Several weld tests were carried out in efforts to develop end-cap welding parameters for the U-Mo corrosion test samples. The main considerations are 1) weld uniformity to prevent water from reaching the exposed U-Mo fuel meat at the end of the rod, and 2) control of the weld depth to prevent U-Mo melting beneath the weld zone. Ideally, the weld would penetrate into the outer stainless steel clad without involving the Nb inner clad layer, which is there to prevent a U-Fe eutectic from forming.

The first series of welds was to practice welding a stainless steel sleeve on a steel rod of approximately the same diameter as the TE1 rod diameter. These images are shown in Figure 5.7 and are characterized in Table 5.2. The lower power welds are just fine for this application but it was decided to perform a better mockup of the actual weld by using two sleeves of stainless steel over a stainless steel rod. This actually worked less realistically since the sleeves buckled during the welding and pulled away from the central rod. These welds are shown in cross-section in Figure 5.8. Table 5.3 lists the weld parameters and weld bead length. Based on this study, end caps are being designed to fit the TE1 nose end (Figure 5.6) and practice welds will be made using the lower power settings.

Table 5.2. Weld dimensions for weld study #1.

Weld Number	Depth of Penetration (μm)	Weld Bead Length (μm)
1	420 (16.5 mils)	1259 (50 mils)
2	520 (20.5 mils)	2282 (90 mils)
3	934 (36.8 mils)	2178 (86 mils)

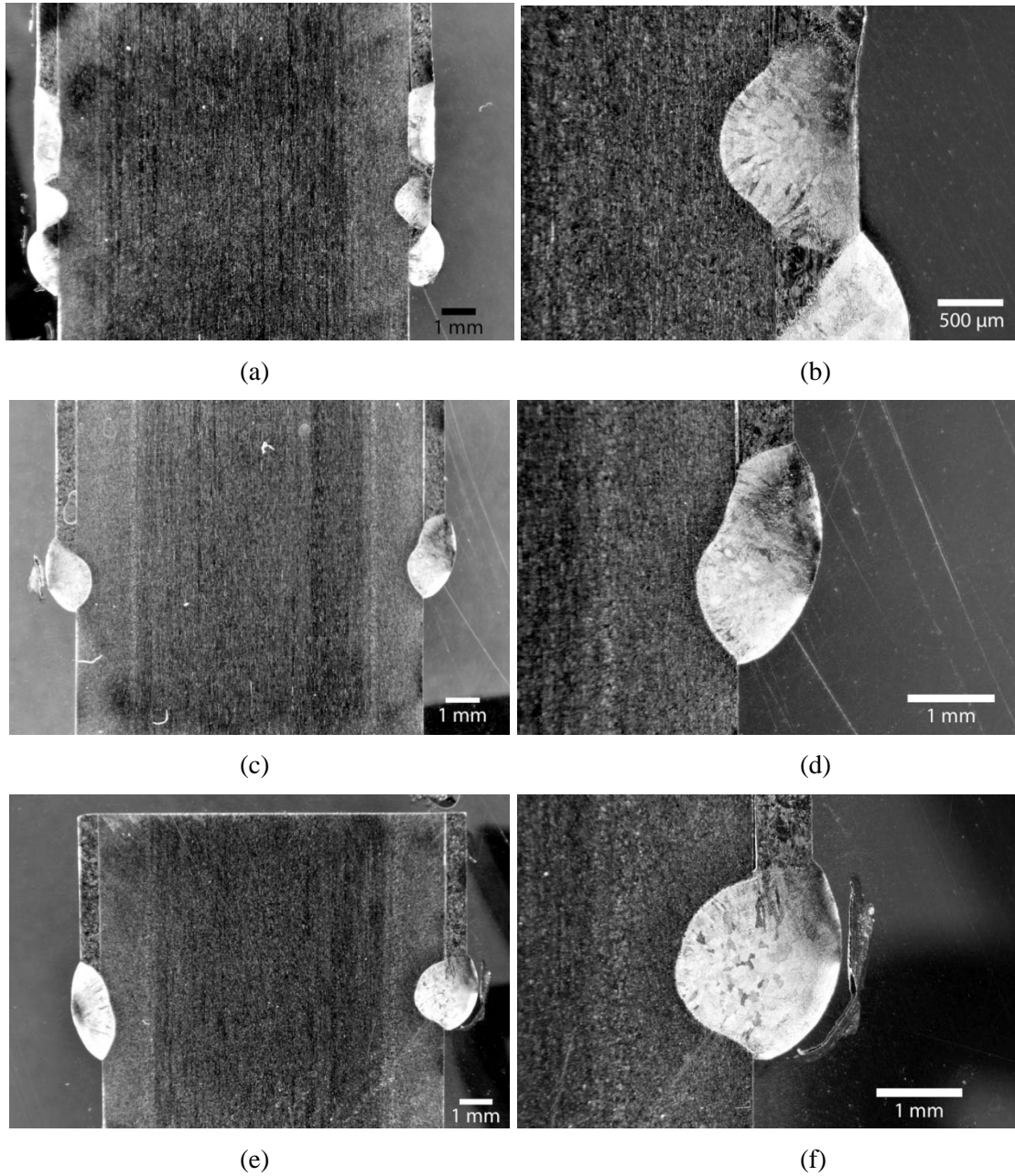


Figure 5.7. Basic images of weld development tests on stainless steels. Low power in (a)-(b), medium power in (c)-(d), and high power in (e)-(f).

The welds appear to be adequate in terms of joining the steels. The depth of penetration is appropriate for Weld #1 if it penetrated the outer steel layer and perhaps goes into the Nb layer without penetrating into the U-10Mo fuel meat. The additional weld testing is shown in Figure 5.8 for 6 different welds. Two steel sleeves were nested over a steel rod to simulate the outer steel clad layer (inner sleeve) welded to a steel end cap (outer sleeve) with the inner steel rod simulating the U-Mo fuel meat. Three power levels, (30, 25, and 22 A) settings using two rotational speeds (2.5 RPM and 3 RPM), gave welding transit times of 9s and 7.2s, respectively.

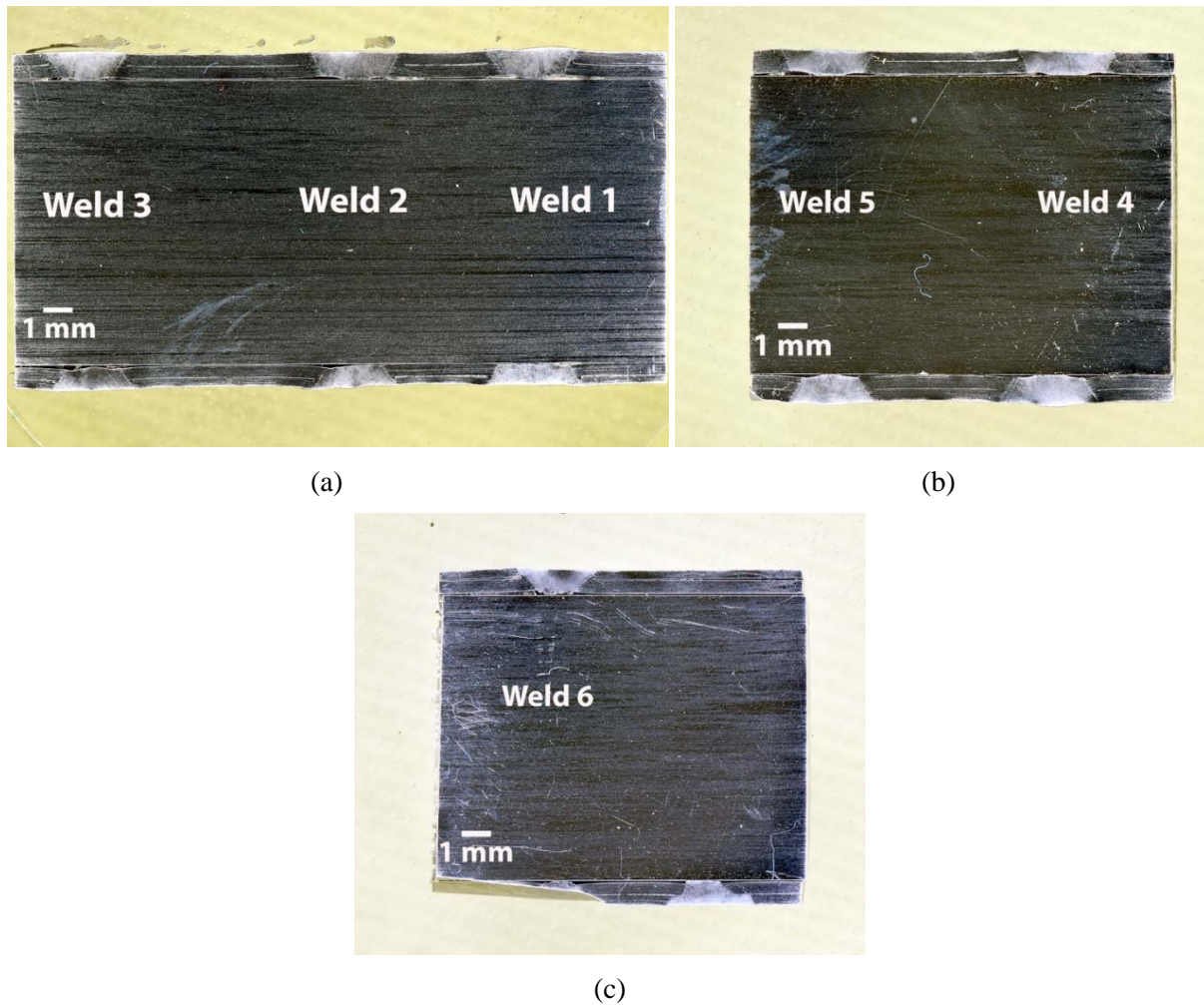


Figure 5.8. Cross-sections of the six welds studied in the second weld test series. Shown in order from top to bottom are welds 1-3 in (a), welds 4 and 5 in (b) and weld 6 in (c).

The welds were then arranged and shown in Figure 5.9 side by side at higher magnification with the same power level and different rotational speeds or transit times for better comparison. All the welds penetrate both steel sleeves but Weld 6A is preferred since it has the smallest surface weld bead width. Lower power and faster rotational speed appears to give a better weld for the purposes of end cap sealing without compromising the U-10Mo fuel meat or inner Nb layer.

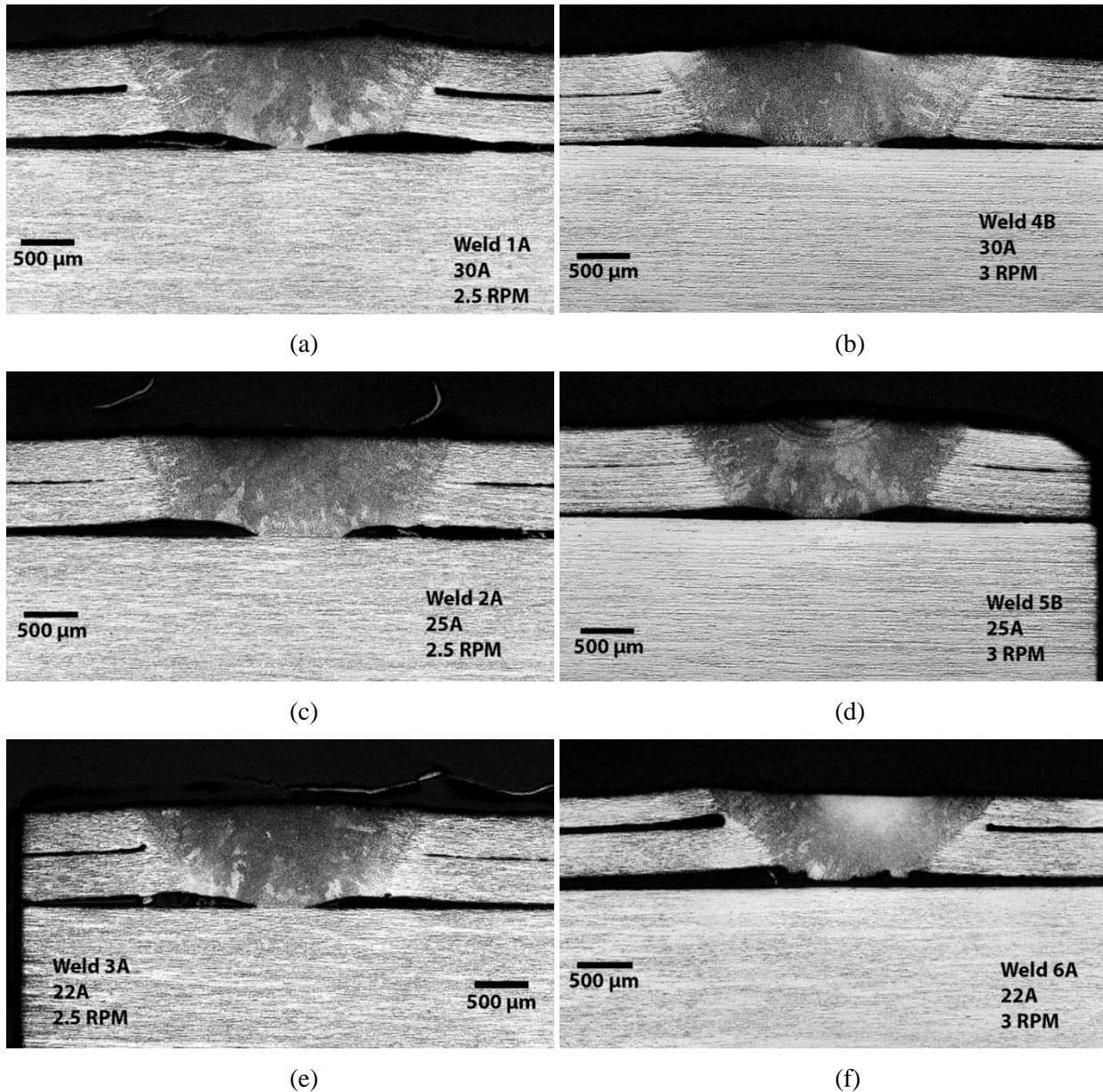


Figure 5.9. The second weld test series using two steel sleeves over a solid steel rod. Shown in (a) through (c) are cross-sections of the welds at 30, 25, and 22 A, respectively with the two rotational speeds of 2.5 RPM and 3 RPM going left to right. Note that in all cases the faster welds are more compact with a finer-grained weld bead.

Table 5.3. Weld parameters and resultant dimensions for weld study #2.

Weld Number	Weld Parameters	Weld Bead Length on Surface (mm)
1A	30A, 2.5 RPM	3.15
4B	30A, 3 RPM	3.3
2A	25A, 2.5 RPM	3.0
5B	25A, 3 RPM	2.8
3A	22A, 2.5 RPM	2.9
6A	22A, 3 RPM	2.7

5.3 End Cap Welded U-Mo Test Sample

The 1-inch long nose end section of TE1 was fitted for end caps, as shown in Figure 5.10 and the end caps were welded onto the TE1 section using a welding apparatus shown in Figure 5.11. The weld parameters chosen from the weld testing were used to minimize the possibility of weld penetration into the U-Mo center.

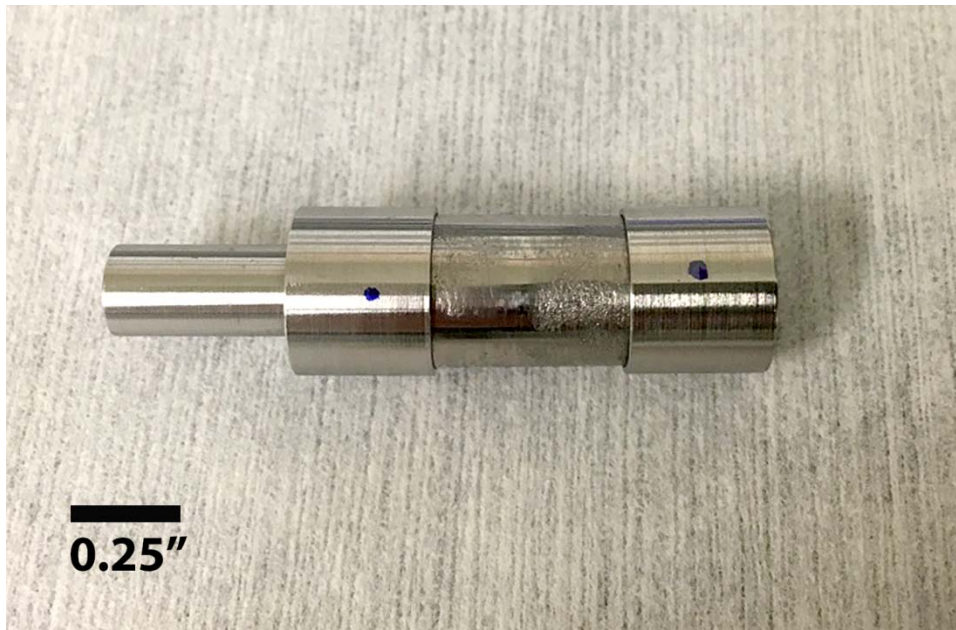


Figure 5.10. Extrusion sample fitted with end caps prior to welding.

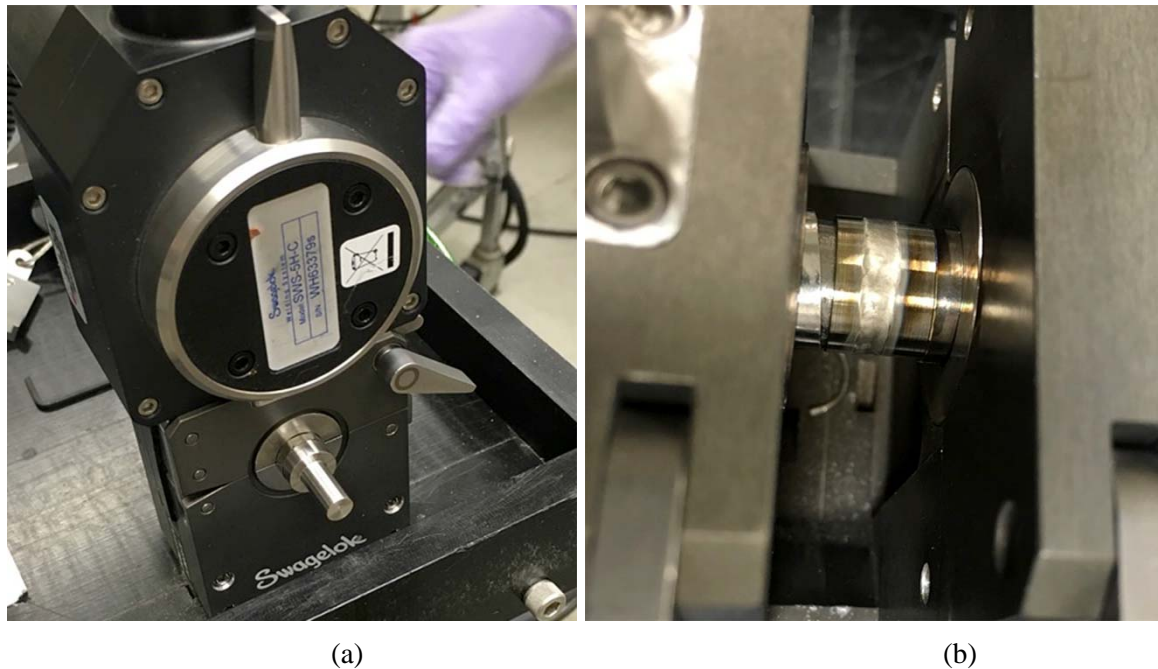


Figure 5.11. (a) Sample in welding fixture ready to be welded and (b) first weld.

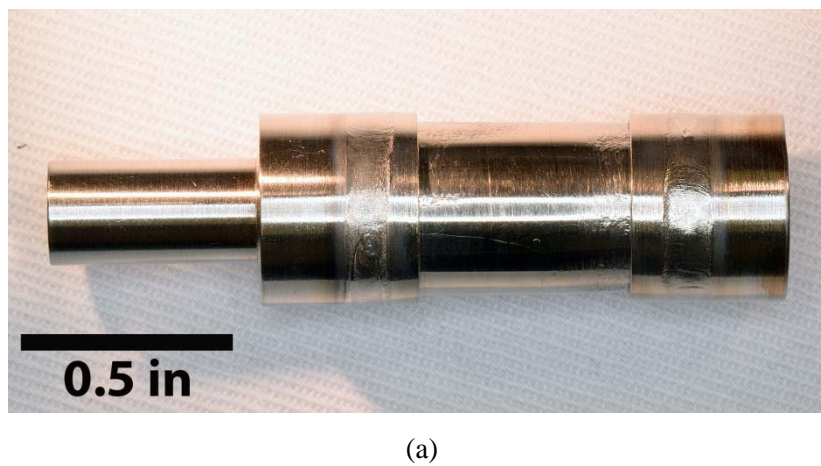


Figure 5.12. OM images of welded test sample from TE1 ready to go into the autoclave test for weld integrity testing. The welds passed a He leak test and were cleaned.

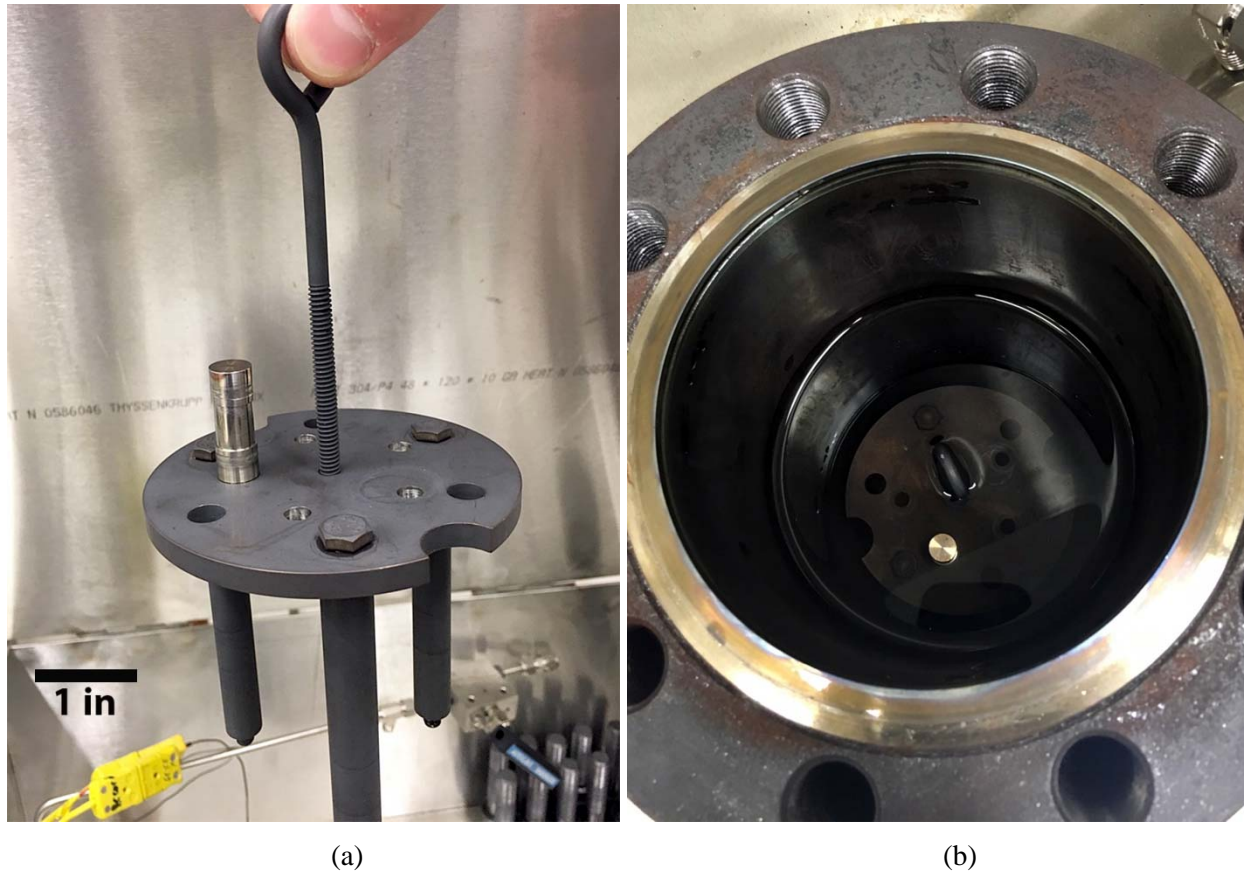
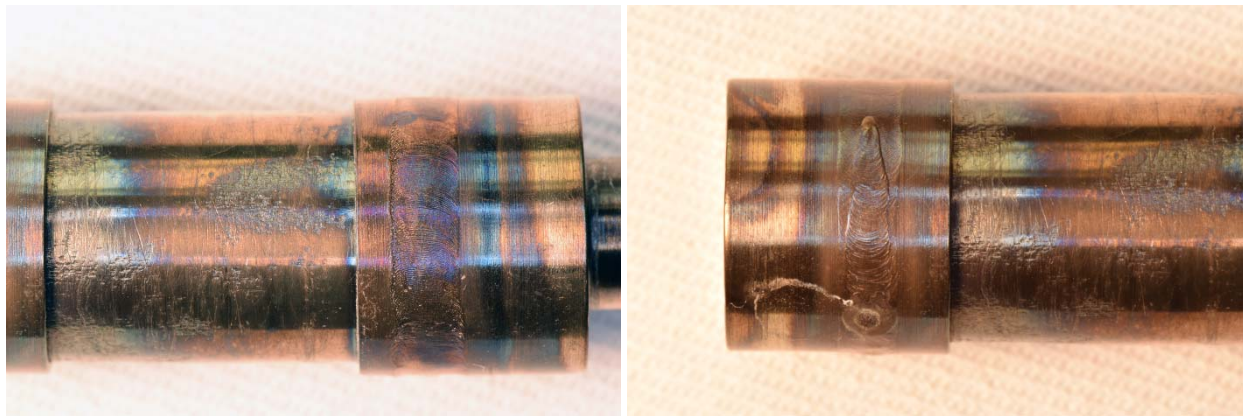


Figure 5.13. (a) Welded TE1 test sample loaded into the autoclave using specimen holder stand and (b) sample and holder stand placed in autoclave in water before autoclave is sealed.

The sample was tested in the autoclave for 165 hours at $300.5^{\circ}\text{C} \pm 0.5^{\circ}\text{C}$ and 1245 psi. It was safely removed and there was no observable contamination in the water of the autoclave or of any part of the autoclave. Normal corrosion of the steel was observed as shown in Figure 5.14. The starting mass of this test sample was 40.883 g and the final mass was 40.955 g, which is a weight gain of 72 mg, probably due to oxidation of the stainless steel surface.



(a)



(c)

(d)

Figure 5.14. OM images of TE1 test sample after 165 hours in autoclave at 300°C and 1245 psi in prototypical pressurized water reactor water.

5.4 Defected Cladding for TE1 First Test

The initial corrosion test consists of an integral fuel/liner/cladding test to examine the effectiveness of the fuel and clad system in the presence of a cladding defect. This proof-of-principle test uses the welded TE1 specimen containing a drilled defect that penetrates the outer cladding but does not penetrate the Nb liner. The sample is being exposed to high temperature and pressure water containing dissolved boron and lithium for 1000 hours. Figure 5.15 to Figure 5.17 detail the creation of a prototypical surface cladding defect for the purposes of this first preliminary and initial corrosion test. Although TE1 does not represent the final specimen design it will be very instructive for these corrosion tests in the future.

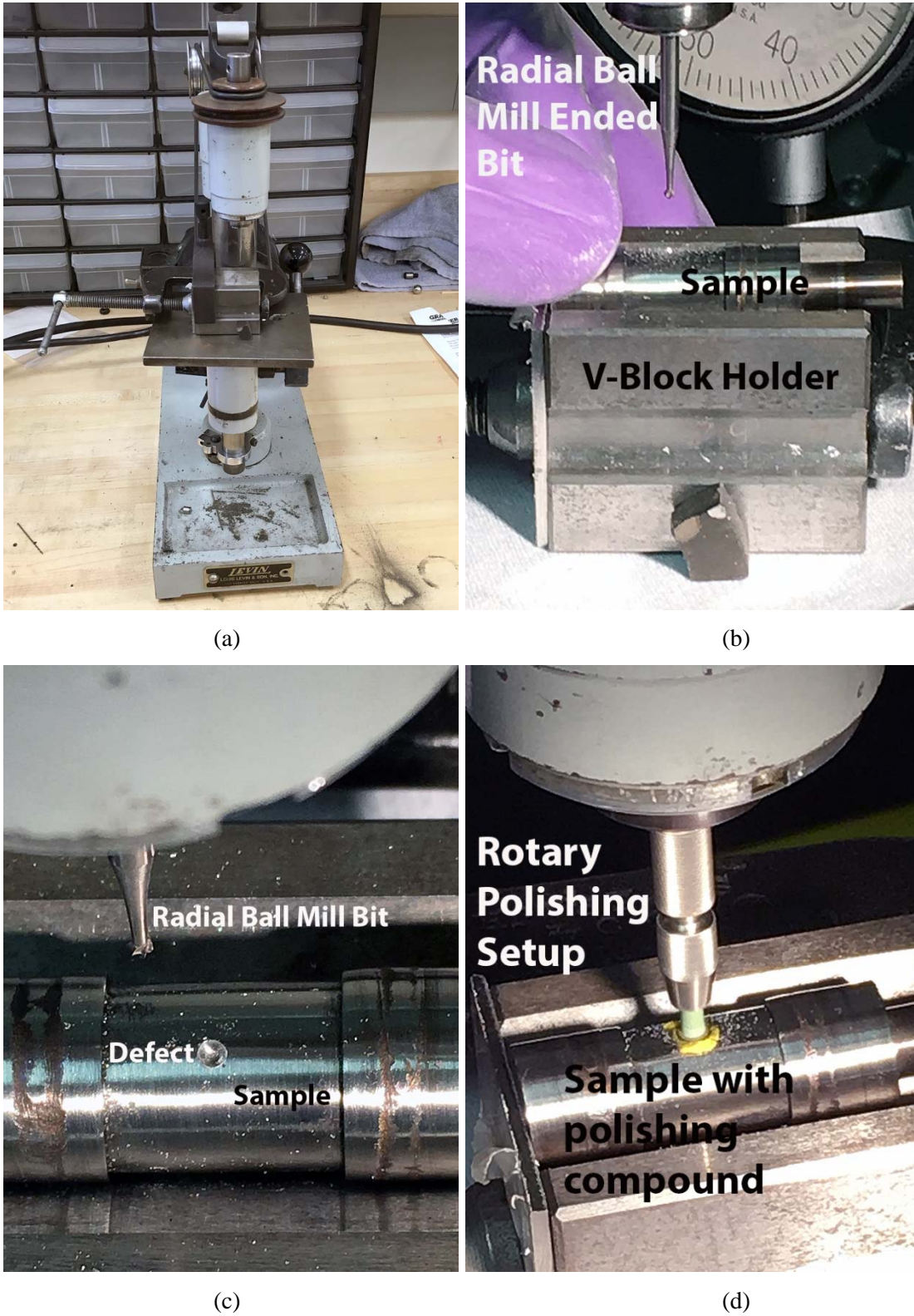


Figure 5.15. (a) Images of (a) rotary drill press, (b) V-block sample holder and radial bit, (c) radial ball mill defect and (d) rotary polishing setup to polish the defect to remove machining burrs and flakes.

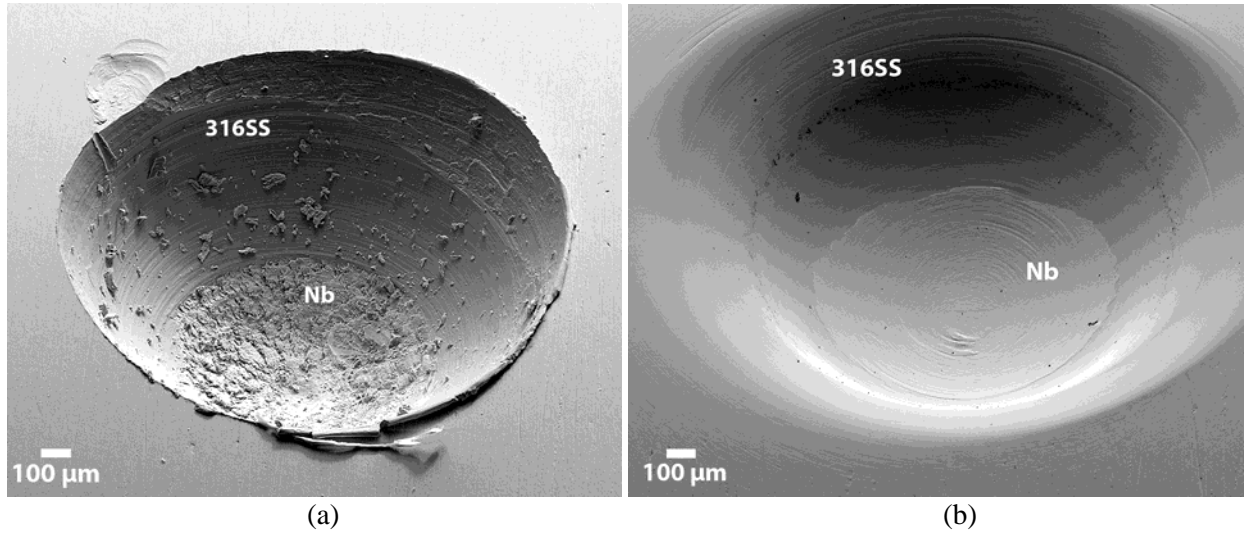


Figure 5.16. (a) Scanning electron microscope (SEM) image of cladding defect (dimple) after radial bit exposes the Nb inner layer and (b) SEM image the same defect after final polishing with 1-μm polishing compound in rotary polishing setup. The various regions are labeled.

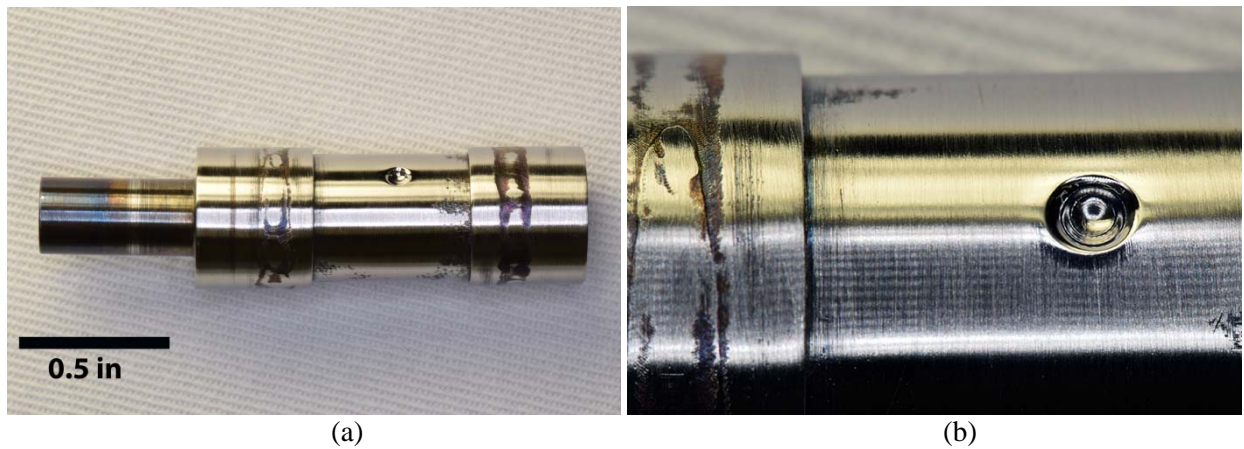


Figure 5.17. OM images of defected (dimpled) test sample from TE1 ready to go into the autoclave test for corrosion testing for 1000 hours at 300°C and 1245 psi. The images show (a) a low magnification of finished test sample and (b) a higher magnification image of simulated cladding defect (dimple). The starting mass of the dimpled test sample from TE1 was 40.9072.

6. BIBLIOGRAPHY

1. Laue K (Formerly Director of Vereinigte Deutsche Metallwerke, Frankfurt, Germany) and H Stenger (Technical Director of Glyco do Brasil Industria Metallurgica, Ltda. Cataguases, Brazil). 1981. "Extrusion" (copyright in English), published in U.S. by American Society for Metals.
 2. Cohen, I., et al., "Development and Properties of Uranium-Base Alloys Corrosion Resistant in High Temperature Water - Part II – Alloys with Protective Cladding", Westinghouse Electric Corporation, WAPD-127, (September 1955).
-